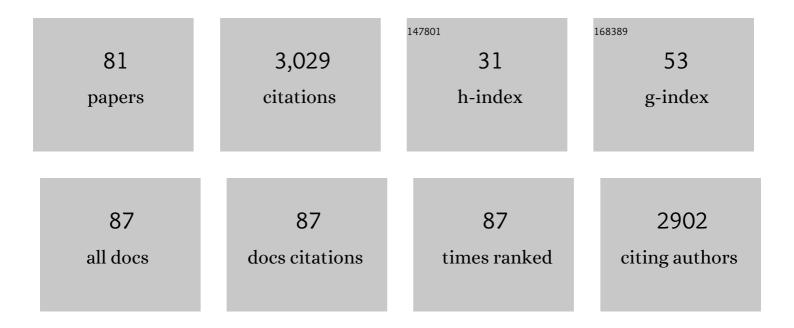
List of Publications by Year in descending order

Source: https://exaly.com/author-pdf/3670495/publications.pdf Version: 2024-02-01



#	Article	IF	CITATIONS
1	Multifunctional Separator Allows Stable Cycling of Potassium Metal Anodes and of Potassium Metal Batteries (Adv. Mater. 7/2022). Advanced Materials, 2022, 34, .	21.0	1
2	A Heterogeneous Palladium Catalyst for the Polymerization of Olefins Prepared by Halide Abstraction Using Surface R ₃ Si ⁺ Species. Angewandte Chemie, 2022, 134, .	2.0	7
3	Hybrid quantum-classical simulations of magic angle spinning dynamic nuclear polarization in very large spin systems. Journal of Chemical Physics, 2022, 156, 124112.	3.0	10
4	Determining the Three-Dimensional Structures of Silica-Supported Metal Complexes from the Ground Up. Inorganic Chemistry, 2022, 61, 1067-1078.	4.0	8
5	Methyl-Driven Overhauser Dynamic Nuclear Polarization. Journal of Physical Chemistry Letters, 2022, 13, 4000-4006.	4.6	13
6	Evolution of structure and transport properties of the Ba8Cu16P30 clathrate-I framework with the introduction of Ga. Applied Physics Letters, 2022, 120, .	3.3	2
7	Efficiency analysis of helium-cooled MAS DNP: case studies of surface-modified nanoparticles and homogeneous small-molecule solutions. Physical Chemistry Chemical Physics, 2021, 23, 4919-4926.	2.8	9
8	Phase-sensitive γ-encoded recoupling of heteronuclear dipolar interactions and 1H chemical shift anisotropy. Solid State Nuclear Magnetic Resonance, 2021, 111, 101712.	2.3	3
9	Catalytic carbon-carbon bond cleavage and carbon-element bond formation give new life for polyolefins as biodegradable surfactants. CheM, 2021, 7, 1347-1362.	11.7	50
10	Revealing the Configuration and Conformation of Surface Organometallic Catalysts with DNP-Enhanced NMR. Journal of Physical Chemistry C, 2021, 125, 13433-13442.	3.1	11
11	Determination of the chemical shift tensor anisotropy and asymmetry of strongly dipolar coupled protons under fast MAS. Solid State Nuclear Magnetic Resonance, 2021, 114, 101743.	2.3	11
12	Direct determination of cellulosic glucan content in starch-containing samples. Cellulose, 2021, 28, 1989-2002.	4.9	12
13	Observing the three-dimensional dynamics of supported metal complexes. Inorganic Chemistry Frontiers, 2021, 8, 1416-1431.	6.0	9
14	High Field Solid-State NMR of Challenging Nuclei in Inorganic Systems. , 2021, , .		1
15	Third time's the charm: intricate non-centrosymmetric polymorphism in <i>Ln</i> SiP ₃ (<i>Ln</i> = La and Ce) induced by distortions of phosphorus square layers. Dalton Transactions, 2021, 50, 6463-6476.	3.3	15
16	Synthesis-enabled exploration of chiral and polar multivalent quaternary sulfides. Chemical Science, 2021, 12, 14718-14730.	7.4	16
17	Site-Specific Sodiation Mechanisms of Selenium in Microporous Carbon Host. Nano Letters, 2020, 20, 918-928.	9.1	30
18	Catalytic upcycling of high-density polyethylene via a processive mechanism. Nature Catalysis, 2020, 3, 893-901.	34.4	262

#	Article	IF	CITATIONS
19	Dynamic Nuclear Polarization of Metal-Doped Oxide Glasses: A Test of the Generality of Paramagnetic Metal Polarizing Agents. Journal of Physical Chemistry C, 2020, 124, 23126-23133.	3.1	12
20	Combining fast magic angle spinning dynamic nuclear polarization with indirect detection to further enhance the sensitivity of solid-state NMR spectroscopy. Solid State Nuclear Magnetic Resonance, 2020, 109, 101685.	2.3	22
21	<i>t</i> ₁ -Noise eliminated dipolar heteronuclear multiple-quantum coherence solid-state NMR spectroscopy. Physical Chemistry Chemical Physics, 2020, 22, 20815-20828.	2.8	31
22	Full-Scale Ab Initio Simulation of Magic-Angle-Spinning Dynamic Nuclear Polarization. Journal of Physical Chemistry Letters, 2020, 11, 5655-5660.	4.6	24
23	Two-step conversion of Kraft lignin to nylon precursors under mild conditions. Green Chemistry, 2020, 22, 4676-4682.	9.0	25
24	Surface Termination of CsPbBr ₃ Perovskite Quantum Dots Determined by Solid-State NMR Spectroscopy. Journal of the American Chemical Society, 2020, 142, 6117-6127.	13.7	135
25	Activation of Low-Valent, Multiply M–M Bonded Group VI Dimers toward Catalytic Olefin Metathesis via Surface Organometallic Chemistry. Organometallics, 2020, 39, 1035-1045.	2.3	8
26	Shedding light on the atomic-scale structure of amorphous silica–alumina and its Brønsted acid sites. Physical Chemistry Chemical Physics, 2019, 21, 19529-19537.	2.8	32
27	Linear-scaling <i>ab initio</i> simulations of spin diffusion in rotating solids. Journal of Chemical Physics, 2019, 151, 034110.	3.0	9
28	High-Field Magic Angle Spinning Dynamic Nuclear Polarization Using Radicals Created by Î ³ -Irradiation. Journal of Physical Chemistry Letters, 2019, 10, 4770-4776.	4.6	19
29	Condensed Phase Deactivation of Solid BrÃ,nsted Acids in the Dehydration of Fructose to Hydroxymethylfurfural. ACS Catalysis, 2019, 9, 11568-11578.	11.2	19
30	Upcycling Single-Use Polyethylene into High-Quality Liquid Products. ACS Central Science, 2019, 5, 1795-1803.	11.3	283
31	Electrophilic Organoiridium(III) Pincer Complexes on Sulfated Zirconia for Hydrocarbon Activation and Functionalization. Journal of the American Chemical Society, 2019, 141, 6325-6337.	13.7	38
32	The anomalous solidification of concrete grindings from acid treatment. Cement and Concrete Research, 2019, 116, 65-69.	11.0	1
33	Enhanced 1H-X D-HMQC performance through improved 1H homonuclear decoupling. Solid State Nuclear Magnetic Resonance, 2019, 98, 12-18.	2.3	11
34	Chemoselective Hydrogenation with Supported Organoplatinum(IV) Catalyst on Zn(II)-Modified Silica. Journal of the American Chemical Society, 2018, 140, 3940-3951.	13.7	56
35	Evidence for Redox Mechanisms in Organometallic Chemisorption and Reactivity on Sulfated Metal Oxides. Journal of the American Chemical Society, 2018, 140, 6308-6316.	13.7	34
36	Synthesis of Supported Pd ⁰ Nanoparticles from a Single-Site Pd ²⁺ Surface Complex by Alkene Reduction. Chemistry of Materials, 2018, 30, 1032-1044.	6.7	17

#	Article	IF	CITATIONS
37	Direct ¹⁷ 0 dynamic nuclear polarization of single-site heterogeneous catalysts. Chemical Communications, 2018, 54, 3472-3475.	4.1	26
38	Optimal sample formulations for DNP SENS: The importance of radical-surface interactions. Current Opinion in Colloid and Interface Science, 2018, 33, 9-18.	7.4	42
39	Large-scale <i>ab initio</i> simulations of MAS DNP enhancements using a Monte Carlo optimization strategy. Journal of Chemical Physics, 2018, 149, 154202.	3.0	22
40	Surface Organometallic Chemistry of Supported Iridium(III) as a Probe for Organotransition Metal–Support Interactions in C–H Activation. ACS Catalysis, 2018, 8, 5363-5373.	11.2	29
41	Characterizing Substrate–Surface Interactions on Alumina-Supported Metal Catalysts by Dynamic Nuclear Polarization-Enhanced Double-Resonance NMR Spectroscopy. Journal of the American Chemical Society, 2017, 139, 2702-2709.	13.7	59
42	Natural Abundance ¹⁷ O DNPâ€NMR Provides Precise Oâ^'H Distances and Insights into the BrÃ,nsted Acidity of Heterogeneous Catalysts. Angewandte Chemie - International Edition, 2017, 56, 9165-9169.	13.8	63
43	Natural Abundance 17 O DNP NMR Provides Precise Oâ^'H Distances and Insights into the BrÃ,nsted Acidity of Heterogeneous Catalysts. Angewandte Chemie, 2017, 129, 9293-9297.	2.0	10
44	Observation of CHâ‹â‹i€ Interactions between Methyl and Carbonyl Groups in Proteins. Angewandte Chemie - International Edition, 2017, 56, 7564-7567.	13.8	17
45	Observation of CHâ‹â‹ï€ Interactions between Methyl and Carbonyl Groups in Proteins. Angewandte Chemie, 2017, 129, 7672-7675.	2.0	5
46	In Silico Design of DNP Polarizing Agents: Can Current Dinitroxides Be Improved?. ChemPhysChem, 2017, 18, 2279-2287.	2.1	32
47	Atomic-Level Structure Characterization of Biomass Pre- and Post-Lignin Treatment by Dynamic Nuclear Polarization-Enhanced Solid-State NMR. Journal of Physical Chemistry A, 2017, 121, 623-630.	2.5	57
48	Improved strategies for DNP-enhanced 2D 1H-X heteronuclear correlation spectroscopy of surfaces. Solid State Nuclear Magnetic Resonance, 2017, 87, 38-44.	2.3	27
49	Innentitelbild: Natural Abundance ¹⁷ O DNPâ€NMR Provides Precise Oâ^'H Distances and Insights into the BrAnsted Acidity of Heterogeneous Catalysts (Angew. Chem. 31/2017). Angewandte Chemie, 2017, 129, 9032-9032.	2.0	0
50	Magnetic resonance imaging of DNP enhancements in a rotor spinning at the magic angle. Journal of Magnetic Resonance, 2016, 264, 125-130.	2.1	10
51	Probing Surface Hydrogen Bonding and Dynamics by Natural Abundance, Multidimensional, ¹⁷ 0 DNP-NMR Spectroscopy. Journal of Physical Chemistry C, 2016, 120, 11535-11544.	3.1	65
52	DNP-Enhanced Ultrawideline Solid-State NMR Spectroscopy: Studies of Platinum in Metal–Organic Frameworks. Journal of Physical Chemistry Letters, 2016, 7, 2322-2327.	4.6	77
53	Identifying low-coverage surface species on supported noble metal nanoparticle catalysts by DNP-NMR. Chemical Communications, 2016, 52, 1859-1862.	4.1	36
54	Effects of biradical deuteration on the performance of DNP: towards better performing polarizing agents. Physical Chemistry Chemical Physics, 2016, 18, 65-69.	2.8	34

#	Article	IF	CITATIONS
55	Quantitative structure parameters from the NMR spectroscopy of quadrupolar nuclei. Pure and Applied Chemistry, 2016, 88, 95-111.	1.9	10
56	Sterically Driven Olefin Metathesis: The Impact of Alkylidene Substitution on Catalyst Activity. Organometallics, 2016, 35, 691-698.	2.3	30
57	High sensitivity and resolution in ⁴³ Ca solid-state NMR experiments. Canadian Journal of Chemistry, 2015, 93, 799-807.	1.1	18
58	Natural Abundance ¹⁷ O DNP Two-Dimensional and Surface-Enhanced NMR Spectroscopy. Journal of the American Chemical Society, 2015, 137, 8336-8339.	13.7	126
59	Zero Thermal Expansion in ZrMgMo ₃ O ₁₂ : NMR Crystallography Reveals Origins of Thermoelastic Properties. Chemistry of Materials, 2015, 27, 2633-2646.	6.7	90
60	Spying on the boron–boron triple bond using spin–spin coupling measured from ¹¹ B solid-state NMR spectroscopy. Chemical Science, 2015, 6, 3378-3382.	7.4	47
61	PRESTO polarization transfer to quadrupolar nuclei: implications for dynamic nuclear polarization. Physical Chemistry Chemical Physics, 2015, 17, 22616-22622.	2.8	33
62	Dynamic Nuclear Polarization Solid-State NMR in Heterogeneous Catalysis Research. ACS Catalysis, 2015, 5, 7055-7062.	11.2	160
63	Solid-state ^{185/187} Re NMR and GIPAW DFT study of perrhenates and Re ₂ (CO) ₁₀ : chemical shift anisotropy, NMR crystallography, and a metal–metal bond. Physical Chemistry Chemical Physics, 2015, 17, 10118-10134.	2.8	18
64	²³ Na magic-angle spinning and double-rotation NMR study of solid forms of sodium valproate. Canadian Journal of Chemistry, 2014, 92, 9-15.	1.1	13
65	Boron–boron <i>J</i> coupling constants are unique probes of electronic structure: a solid-state NMR and molecular orbital study. Chemical Science, 2014, 5, 2428-2437.	7.4	40
66	Theoretical study of homonuclear J coupling between quadrupolar spins: Single-crystal, DOR, and J-resolved NMR. Journal of Magnetic Resonance, 2014, 242, 23-32.	2.1	19
67	Direct Characterization of Metal–Metal Bonds between Nuclei with Strong Quadrupolar Interactions via NMR Spectroscopy. Journal of Physical Chemistry Letters, 2014, 5, 4049-4054.	4.6	21
68	NMR crystallography of sodium diphosphates: combining dipolar, shielding, quadrupolar, diffraction, and computational information. CrystEngComm, 2013, 15, 8727.	2.6	24
69	Symmetry-Amplified <i>J</i> Splittings for Quadrupolar Spin Pairs: A Solid-State NMR Probe of Homoatomic Covalent Bonds. Journal of the American Chemical Society, 2013, 135, 12596-12599.	13.7	31
70	Signal enhancement in solid-state NMR of quadrupolar nuclei. Solid State Nuclear Magnetic Resonance, 2013, 51-52, 1-15.	2.3	58
71	Measuring dipolar and <i>J</i> coupling between quadrupolar nuclei using double-rotation NMR. Journal of Chemical Physics, 2013, 138, 174202.	3.0	34
72	QUEST—QUadrupolar Exact SofTware: A fast graphical program for the exact simulation of NMR and NQR spectra for quadrupolar nuclei. Solid State Nuclear Magnetic Resonance, 2012, 45-46, 36-44.	2.3	77

#	Article	IF	CITATIONS
73	Multinuclear Magnetic Resonance Crystallographic Structure Refinement and Cross-Validation Using Experimental and Computed Electric Field Gradients: Application to Na ₂ Al ₂ B ₂ O ₇ . Journal of Physical Chemistry C, 2012, 116, 19472-19482.	3.1	52
74	Potent inhibition of ice recrystallization by low molecular weight carbohydrate-based surfactants and hydrogelators. Chemical Science, 2012, 3, 1408.	7.4	102
75	23Na double-rotation NMR of sodium nucleotides leads to the discovery of a new dCMP hendecahydrate. Physical Chemistry Chemical Physics, 2012, 14, 4677.	2.8	18
76	Sodium-23 Ssolid-Sstate Snuclear Smagnetic Sresonance of Scommercial Ssodium Snaproxen and its Ssolvates. Journal of Pharmaceutical Sciences, 2012, 101, 2930-2940.	3.3	39
77	Direct Investigation of Covalently Bound Chlorine in Organic Compounds by Solidâ€State ³⁵ Clâ€NMR Spectroscopy and Exact Spectral Lineâ€Shape Simulations. Angewandte Chemie - International Edition, 2012, 51, 4227-4230.	13.8	69
78	A ZORA-DFT and NLMO study of the one-bond fluorine–X indirect nuclear spin-spin coupling tensors for various VSEPR geometries. Canadian Journal of Chemistry, 2011, 89, 789-802.	1.1	2
79	Removal of sidebands in double-rotation NMR in real time. Journal of Magnetic Resonance, 2011, 211, 234-239.	2.1	3
80	Residual dipolar coupling between quadrupolar nuclei under magic-angle spinning and double-rotation conditions. Journal of Magnetic Resonance, 2011, 213, 82-89.	2.1	21
81	Measurement of Δ1J(199Hg, 31P) in [HgPCy3(OAc)2]2 and relativistic ZORA DFT investigations of mercury–phosphorus coupling tensors. Solid State Nuclear Magnetic Resonance, 2009, 36, 182-191.	2.3	13